Competition Between Hydrotreating and Polymerization Reactions During Pyrolysis Oil Hydrodeoxygenation

F. De Miguel Mercader and P. J. J. Koehorst
Thermo-Chemical Conversion of Biomass Group, Research Institute IMPACT, Faculty of Science and Technology, University of Twente, 7500AE Enschede, The Netherlands

H.J. Heeres
Dept. of Chemical Engineering, Institute of Technology and Management, University of Groningen, 9747 AG Groningen, The Netherlands

S. R. A. Kersten and J. A. Hogendoorn
Thermo-Chemical Conversion of Biomass Group, Research Institute IMPACT, Faculty of Science and Technology, University of Twente, 7500AE Enschede, The Netherlands

DOI 10.1002/aic.12503
Published online February 15, 2011 in Wiley Online Library (wileyonlinelibrary.com).

Hydrodeoxygenation (HDO) of pyrolysis oil is an upgrading step that allows further coprocessing of the oil product in (laboratory-scale) standard refinery units to produce advanced biofuels. During HDO, desired hydrotreating reactions are in competition with polymerization reactions that can lead to unwanted product properties. To suppress this polymerization, a low-temperature HDO step, referred to as stabilization, is typically used. Small batch autoclaves have been used to study at near isothermal conditions the competition between hydrotreating and polymerization reactions. Although fast polymerization reactions take place above 200°C, hydrogen consumption was already observed for temperatures as low as 80°C. Hydrogen consumption increased with temperature and reaction time; however, when the end temperature exceeded 250°C, hydrogen consumption achieved a plateau. This was thought to be caused by the occurrence of fast polymerization reactions and the refractivity of the products to further hydrotreating reactions. The effect of the gas–liquid mass transfer was evaluated by using different stirring speeds. The results of these experiments (carried out at 300°C) showed that in the first 5 min of HDO, gas–liquid mass transfer appears to be limiting the overall rate of hydrotreating reactions, leading to undesired polymerization reactions and product deterioration. Afterward, intraparticle mass transfer/kinetics seems to be governing the hydrogen consumption rate. Estimations on the degree of utilization (effectiveness factor) for industrially sized catalysts show that this is expected to be much lower than 1, at least, in the early stage of HDO (first 30 min). Catalyst particle size should, thus, be carefully considered when designing industrial processes not only to minimize reactor volume but also to improve the ratio of hydrotreating to polymerization reactions. © 2011 American Institute of Chemical Engineers *AIChE J,* 57: 3160–3170, 2011

Correspondence concerning this article should be addressed to J. A. Hogendoorn at j.a.hogendoorn@utwente.nl.

Keywords: pyrolysis oil, upgrading, hydrodeoxygenation, polymerization, mass transfer, absorption

Introduction

Hydrodeoxygenation (HDO) of pyrolysis oil is an upgrading step that allows coprocessing of biomass products with fossil feed in (laboratory-scale) standard refinery units.[1–3] During HDO, pyrolysis oil is treated at temperatures between 150 and 450°C, high hydrogen pressures (5–25 MPa), and in the presence of an active catalyst. A recent historical overview of the developments in HDO of pyrolysis oil has been written by Elliott in 2007.[4]

Early studies on HDO of pyrolysis oil report that directly processing pyrolysis oil at high temperatures (>300°C) was troublesome, showing coking and plugging of lines.[5] For that reason, a low-temperature HDO step (referred to as stabilization) was introduced, probably reducing the reactivity (toward polymerization/polycondensation reactions) of functional groups such as aldehydes, ketones, and double C=C bonds.[6] In this way, successful HDO operation at high temperature was feasible, achieving higher deoxygenation levels (typically > 95%).[7,8]

In our previous study on HDO,[1] experiments were carried out in a batch autoclave at 29 MPa total pressure (20 MPa H_2 initial), 230–340°C end temperature, and 5 wt % Ru/C catalyst. Heating rates in the autoclave were very low; it typically took 1.5–2 h to reach the desired end temperature. The total reaction time (after heating to the desired temperature) was 4 h, after which the reactor was cooled. For all the experiments, more than 50% of the hydrogen consumption took place during the heating time. Therefore, the low-temperature stabilization reactions were an integrated part of the experiments. Compared with the feed, the resulting HDO oil had a lower oxygen content and coking tendency (measured by microcarbon residue test, MCRT), whereas the molecular weight was reduced with increasing temperature. Although the oxygen content of the resulting HDO oils was still relatively high (up to 28 wt % on dry basis), these oils could be coprocessed in laboratory-scale refinery units without any operational problems. Moreover, yields were comparable to the ones obtained when processing fossil feed only.

High-pressure thermal treatment (HPTT) is a process in which pyrolysis oil is subjected to temperatures between 200 and 350°C, pressures higher than 20 MPa, and short residence times (<5 min) in the absence of catalyst and hydrogen.[9] Experiments conducted in a continuous HPTT setup showed that, similar to HDO, the oxygen and water content of the oil product are reduced, increasing its energy density. However, during HPTT and opposite to HDO, pyrolysis oil underwent polymerization shown by a severe increase in molecular weight and viscosity of the oil product. An aqueous phase with the remainder of the organics and some gas (mainly CO_2) were also produced. Although HDO oils could be coprocessed in a laboratory-scale refinery unit, the HPTT oils could not be processed because of their high coking tendency (measured by MCRT), molecular weight, and its immiscibility with fossil feed.

Although both HPTT and HDO can produce an oil with lower and similar oxygen content, other properties are completely different. Moreover, the processes are carried out on completely different timescales. HPTT can lead to a deoxygenated though heavily polymerized product within 2 min, whereas HDO requires much longer reaction times, but produces an oil with a molecular weight distribution (MWD) similar or even lower than the feed.[1] As already seen by the coking of lines during direct high-temperature HDO processing, the polymerization reactions (typical during HPTT) can also be present during HDO. The ''stabilization step" at reduced temperature level is, therefore, aimed to favor the rate of the hydrogenation/hydrodeoxygenation reactions with respect to that of the competing polymerization reactions[5] (see Figure 1 for schematic representation of this competition).

In this article, experimental and theoretical results of the HDO of pyrolysis oil are reported and discussed, specifically addressing the competition between the polymerization and hydrotreating/hydrodeoxygenation reactions in the early stage of the HDO process (first 30 min). Different process conditions (such as stirring intensity, heating time, and reaction temperature) were used to study their effect on the competing reactions and on final product properties.

Model Development of HDO and Polymerization

For the numerical evaluation of experiments in terms of competition between hydro(deoxy)genation and polymerization, several assumptions have to be made. It should be noted that some of these assumptions are rather rough. However, considering that these are just the first steps in modeling the HDO process[10–12] and the fact that this study aims to

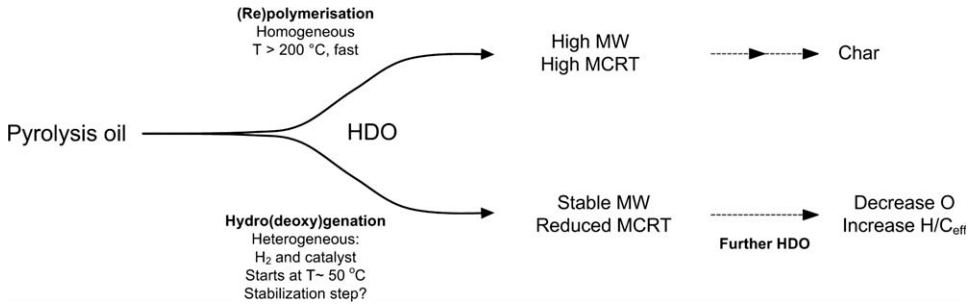

Figure 1. Schematic representation of the competition between polymerization and hydrodeoxygenation reactions.

Table 1. Properties of the Forest Residue Pyrolysis Oil

	Pyrolysis Oil
Elemental composition and water content	
C dry (wt %)	54.3
H dry (wt %)	7.0
O dry (wt %)*	38.7
Water (wt %)	25.0
Carbon residue	
MCRT (wt %)	19.7
MCRT dry† (wt %)	26.2

*By difference.
†Corrected for water content.

validate the scheme in Figure 1 (identifying the parameters/rate-controlling steps that can influence the balance between HDO and polymerization), this is not considered a major drawback.

For the hydrogen-consuming, heterogeneous, reactions, it is assumed that:

- The hydrotreating reactions can only take place at or inside the catalyst.
- Both hydrogen and pyrolysis oil components are assumed to be able to enter the pores of the porous catalyst particles to react at the internal surface area.
- Although pyrolysis oil is a mixture of many different components, with each of them having its own hydro(deoxy)genation reaction mechanism and corresponding kinetic expression, in this work, a uniform (lumped) kinetic expression for the hydrotreating reactions is used.
- For hydrogen, the reaction order is assumed to be 1 (this has been observed for hydrogenation of benzene[13] and glucose[14]).
- The concentration of reactive pyrolysis oil components is constant. The contribution of pyrolysis oil (components) in the kinetic expression is, thus, lumped into a pseudo-first-order rate constant.
- Reactions are assumed to be irreversible.
- For hydrogen, Fickian diffusion is assumed inside the catalyst pores.

In the present three-phase system, several (serial) resistances can influence the overall hydrogen uptake rate. Considering that in the current experiments the fraction of hydrogen in the gas is high when compared with other noncondensable gases, the H_2 mass-transfer resistance from the gas phase to the gas–liquid interface will be neglected. Moreover, a possible mass-transfer resistance of pyrolysis oil components toward or inside the catalyst will also be neglected. Based on these and the previously mentioned assumptions, the resulting flux equation as used in this study is defined as

$$N_{H_2} = \frac{C_{H_2,G}}{\frac{1}{m.k_L.a_{GL}} + \frac{1}{m.k_S.a_S} + \frac{1}{m.\eta.k_1.\varepsilon_S}} \ (\text{mol m}_{\text{liquid}}^{-3}\ \text{s}^{-1}) \quad (1)$$

From this equation, it can be seen that, for the experimental conditions applied in this study, three resistances for hydrogen consumption have to be taken into account: gas–liquid mass transfer, mass transfer from the bulk of the liquid to the catalyst surface, and apparent kinetics (determined by intrinsic reaction kinetics and simultaneous diffusion inside the catalyst). The relative importance of each resistance can be estimated by (approximate) calculations as will be shown in the following sections.

To prevent product deterioration, the hydrogen uptake rate related to HDO as in Eq. 1 should be at least of the same order of magnitude as the rate of the thermal polymerization reactions. These uncatalyzed polymerization reactions have proven to be very fast during HPTT of pyrolysis oil, creating a polymerized product within 5 min at temperatures above 250°C.[9] When using glucose as model compound in HPTT experiments (De Miguel Mercader et al., submitted for publication), conversion of glucose to a polymerized product at 300°C also occurred within 5 min, whereas experiments conducted at 250°C and 5 min had a (calculated) conversion of only 28 wt %. This illustrates why a HDO pretreatment of pyrolysis oil at temperatures of 150–250°C (stabilization) is typically applied before performing HDO at higher temperatures.

Experimental

Materials

Pyrolysis oil as used in this study was supplied by VTT, Finland, and produced from forest residue. Table 1 shows some properties of this oil. The oil was stored at −10°C to avoid aging. The amount needed for one experiment was brought to room temperature the day before usage.

H_2 and N_2 (both 99.9% purity) were obtained from the high-pressure network in the laboratory, fed by cylinders from Linde gas. CO_2 used to study the gas–liquid mass-transfer characteristics was available at 99.99% purity from Linde gas.

The catalyst used was 5 wt % ruthenium on activated carbon (Ru/C), delivered by Sigma-Aldrich. The average particle size was 14 μm. The use of such small catalyst size is expected to decrease both external and internal mass-transfer resistances. Surface area, pore-size distribution, and pore volume of the catalyst were determined using BET analysis (Table 2). The ruthenium distribution on the surface of the catalyst particles is assumed to be homogeneous, but was not further investigated.

Experimental setups and procedure

Small in-house made autoclaves, with volumes of 9, 40, and 45 ml, were used in this study. During the experiments, the mixing of the contents of the 9- and 40-ml reactor was done by fast shaking of the whole autoclave; the 45-ml reactor used a hollow shaft stirrer (0–48 Hz). The hollow shaft stirrer is expected to improve mass transfer when compared with the shaken autoclaves. These reactors were fixed to a pneumatic arm. The pneumatic arm had an internal piston that allowed the reactors to be immersed in a fluidized sand

Table 2. BET Analysis of the Ru/C Catalyst

	Ruthenium on Carbon Catalyst
BET surface area	810 ± 11 m^2 g^{-1} (total) 579 m^2 g^{-1} (micropores only)
Langmuir surface area	1094 ± 10 m^2 g^{-1}
Pore volume (porosity), ε	0.27 cm^3 g^{-1} STP
Pore size	Most pores between 6 and 12 nm

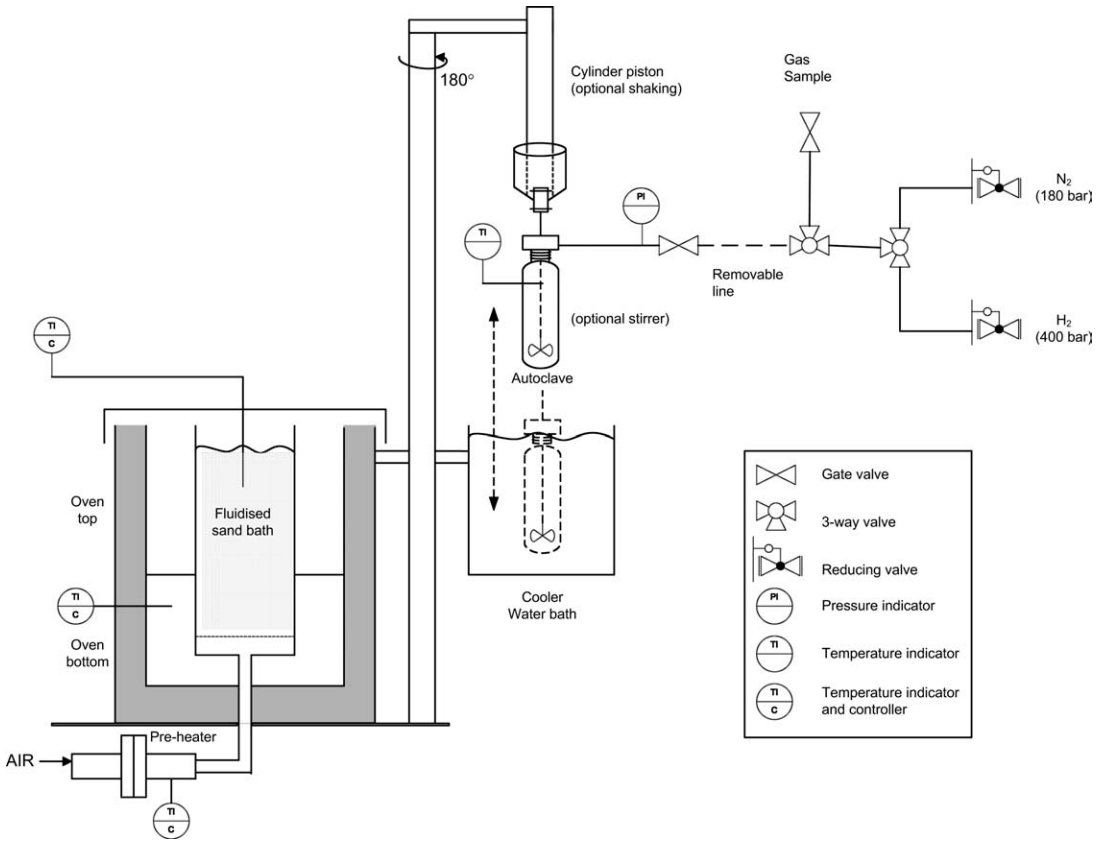

Figure 2. HDO setup diagram.

bed and a cooling bath to obtain fast heating and cooling, respectively (see Figure 2). The fluidized sand bed was heated by two electric ovens with independent temperature controllers. The fluidization gas was preheated by a separate heating element.

In each of the reactors, a thermocouple inside the reactor recorded the inner temperature. Figure 3 shows that the heating rate decreased with reactor volume, but was very quick in all cases compared with the heating rate of the 5-l autoclave used in a previous study by De Miguel Mercader et al.[1]

In a typical experiment, the reactor was filled with the desired amount of pyrolysis oil (reactor filling about 50%) and 5 wt % catalyst. The reactor was then closed tightly and attached to the moving arm. After leak testing with nitrogen, the reactor was purged and filled with 12 MPa of hydrogen. If the reactor was again leak free, the gas line was detached.

At the start of an experiment, the pneumatic arm was moved to the position over the sand bed and then immersed in the bed (which was at constant temperature between 80 and 300°C). For the stirred experiments, stirring was started before heating to presaturate the liquid. For the shaken reactors, shaking was started directly while lowering the reactor into the bed, for the same purpose. After the desired reaction time (from 10 to 60 min), the reactor (both stirred and shaken) was lifted from the hot sand bed, moved over the water bath, and lowered into the cooling water.

After the reactor was cooled to room temperature, pressure was noted and a gas sample was taken for analysis. Then, the reactor was depressurized completely. The liquid sample including the catalyst was collected in a syringe. The reactor walls were scraped with a metal bar to ensure, as much as possible, the recovery of the contents. For the shaken reactors, samples from experiments at higher temperatures (above 200°C) generally were more difficult to collect

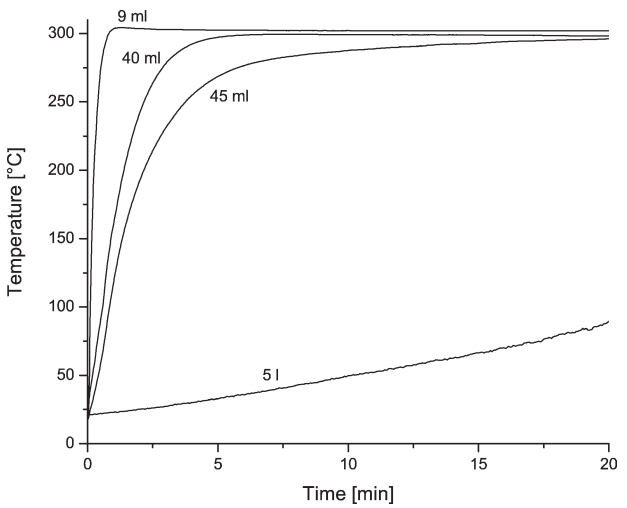

Figure 3. Temperature profile during experiments using different autoclave sizes.

Data for the 5-l reactor correspond to experiment conducted at 300°C shown in Ref. 1.

Table 3. Overview of Experimental Series, Their Goal, and Process Conditions

Series	Reactor/Goal	Conditions
1	Shaken Effect of reaction time and end temperature	9-ml reactor, 5-g liquid 10–30–60 min 80–120–165–200–250–300°C 12 MPa H_2, 5 wt % catalyst
2	Shaken Effect of heating time	9- to 40-ml reactor, 5- to 20-g liquid 30 min 300°C 12 MPa H_2, 5 wt % catalyst
3	Stirred Effect of catalyst holdup	45-ml reactor, 20-g liquid 30 min 300°C 48 Hz stirring 12 MPa H_2, 2.5–5–7.5 wt % catalyst
4	Stirred $k_L.a_{GL}$ estimation	45-ml reactor, 20-g liquid CO_2 absorption in H_2O, 20°C 8.6–48.1 Hz stirring
5	Stirred Effect of stirring speed	45-ml stirred, 20-g liquid 30 min 300°C 0–7–15–48 Hz stirring 12 MPa H_2, 5 wt % catalyst

because of the high viscosity of the resulting liquid product, making liquid analysis impossible.

The collected liquid sample was filtered by attaching a filtration unit with Whatman Grade 3 filter paper (retention from 6 μm) to the syringe and pressing the liquid sample through the filter (manually or by nitrogen pressure).

Separate gas–liquid mass-transfer experiments were carried out to obtain an indication of $k_L.a_{GL}$ in the stirred autoclave. These were performed at 20°C using degassed water and CO_2. The reasons for choosing this system are clarified in the section "Mass-transfer limitations during HDO."

Monitored parameters and analysis methods

Total hydrogen consumption was monitored as key parameter for hydrotreating reactions. To evaluate the extent of polymerization reactions, molecular weight measurements were carried out with an Agilent Technologies HPLC 1200 series using gel permeation chromatography (GPC) columns (more details about this equipment can be found in Ref. 9). The coking tendency of the upgraded oils was measured by MCRT according to ASTM standard D 4530-07 with an ACR-M3 Micro Carbon Residue Tester from Tanaka Scientific. This parameter has been found to correlate well with the MWD of upgraded pyrolysis oil[1,15] and, thus, was also used to evaluate polymerization.

Besides that, various other techniques were used to analyze samples. The water content of samples (used to calculate dry MCRT) was determined by Karl Fischer titration with a Metrohm 787 KF Titrino. Titrations were carried out with hydranal in a 3:1 mixture of methanol and dichloromethane. The composition of the gas samples obtained after the experiments was determined with a Varian CP-4900 microgas chromatograph (for further details see Ref. 9).

Experimental Results and Discussion

Experiments

Experiments were carried out in both shaken and stirred reactors. The shaken reactors were especially used to study the influence of end temperature, reaction time, and heating rate (by using differently sized reactors, the external surface area to internal volumes changed, obtaining different heating rates). The stirred reactor was specifically used to study the influence of stirring rate and catalyst holdup. Various other experiments in the stirred reactor were performed to obtain $k_L.a_{GL}$ values as needed in the numerical interpretation. In Table 3, an overview of the experiments carried out is shown.

Qualitative assessment of results

Temperature Level. In Figure 4, the total hydrogen consumption is shown for the experiments of series 1. The hydrogen consumption was calculated from the difference in initial and final reactor pressure, corrected for produced gases (mainly CO_2 and CH_4). These results show that there was already hydrogen consumption at 80°C, which is in line with previous results.[1,15] Up to a temperature of 200°C, the hydrogen consumption increased with both temperature and reaction time. However, the experiments at 250 and 300°C showed no further increase in hydrogen consumption compared with the experiment at 200°C. This stop in the increase of hydrogen consumption cannot be explained by a possible shortage of hydrogen as only half of the initially present quantity was consumed. Moreover, the maximum hydrogen consumption ($\sim$2.5 mol kg^{-1}_{feed}) is low when compared with the hydrogen consumption in the 5-l autoclave (9.3–13.2 mol kg^{-1}_{feed} for end temperatures of 230–340°C), indicating that HDO reactions can still further consume H_2 when enough time is given to allow the low-temperature stabilization reactions to occur (using, for example, low heating rates). Total catalyst deactivation also cannot explain these results, as an experiment with a reused catalyst

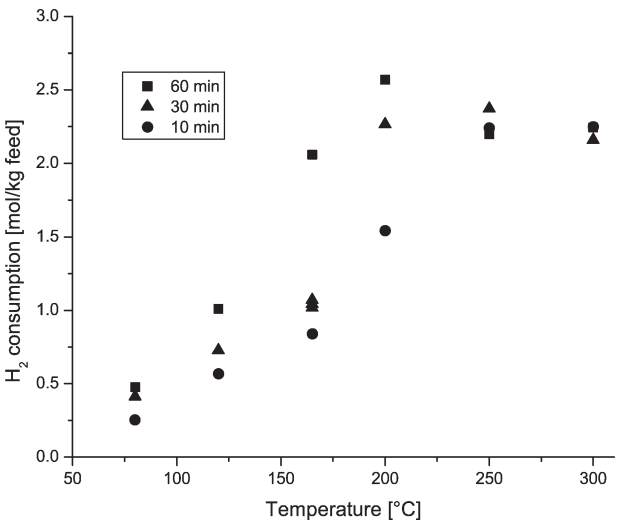

Figure 4. Total hydrogen consumption as a function of temperature and reaction time in the shaken 9-ml autoclave.

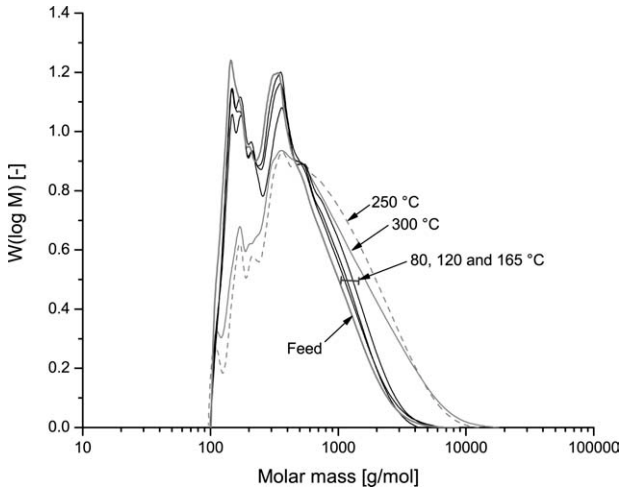

Figure 5. Molecular weight distribution of the oil products after HDO in the 9-ml shaken autoclave using different temperatures.

The reaction time and the initial H_2 pressure were 30 min and 12 MPa, respectively.

still showed considerable activity, although somewhat lower than a fresh catalyst (results not presented). The results at high temperatures might be explained by the expected fast polymerization at and above 250°C leading to a polymerized product that is refractive to further consumption of hydrogen. The occurrence of polymerization also can be deduced from Figure 5, which shows that the oil products produced at 250 and 300°C have higher molecular weight than the products obtained at lower temperature (which have a molecular weight similar to or slightly higher than that of the feed oil).

Heating Rate. The effect of heating rate on the competition between polymerization and hydrotreating was evaluated by using two differently sized reactors (9 and 40 ml), a total reaction time of 30 min, and a temperature of 300°C (series 2, Table 3). The increase in reactor size changed the external heat exchange area to the internal volume, resulting in longer heating times to reach 300°C. This is illustrated in Figure 3 and also quantitatively expressed in Table 4. It should be noted that in all cases the heating rate was very fast, especially when compared with the heating rate in the 5-l autoclave used in the study by De Miguel Mercader et al.[1] The use of differently sized reactors can also influence the mass-transfer characteristics; however, this effect was not explicitly quantified and neglected in the analysis. Although the heating time in both cases was short compared with the reaction time of 30 min (see Figure 3), a shift in the ratio between hydrotreating reactions and polymerization reactions (and thus product properties) was still observed: hydrogen consumption decreased with increasing heating rate (Table 4). As already indicated in the previous sections, these results also suggest that giving less time for low-temperature hydrotreating reactions to occur (by increasing the heating rate from ambient temperature to 300°C), polymerization reactions are increasingly favored and can inhibit hydrotreating reactions.

Table 4. Comparison of Hydrogen Consumption per Kilogram of Feed for Different Reactor Sizes in the Shaken Setup

Reactor Volume (ml)	Heating Rate (°C s^{-1})*	H_2 Consumption (mol kg^{-1}_{feed})
9	7.6	2.16
40	1.3	3.43

The reactions conditions were as follows: 300°C, 5 wt % catalyst, and 30-min reaction time.
*Average to reach 285°C.

The MWD of the resulting oils (Figure 6) confirms this: with increasing heating rate, the average molecular weight increased. For comparison, also the result obtained in a 5-l autoclave experiment at 300°C[1] is given, which (for 300°C end temperature) had a typical heating time of 90 min. This curve shows a distinct shift to the left when compared with feed oil, which indicates that, overall, cracking and not polymerization occurred in that case.

Catalyst Holdup If the mass-transfer resistance to the catalyst particles (Eq. 2) or the apparent kinetics inside the catalysts (Eq. 3) would be the overall rate-controlling step, a proportional relationship between catalyst holdup and hydrogen conversion rate should be observed (if H_2 pressure is constant). Because the experiments were carried out batch wise, a nonstationary gas mass balance should be used to derive the theoretical relationship between average flux (or total hydrogen consumption over a certain time interval) and catalyst holdup. If either of the aforementioned resistances is limiting, the following proportionality can be derived from such balance: $\ln(\eta_{H_2,G}(t\ \text{min})/\eta_{H_2,G}(0)) = -C_1.\varepsilon_s.t$. In the 45-ml autoclave (48 Hz, 30 min), three different catalyst holdups (2.5, 5, and 7.5 wt %) were used to study whether this dependency was observed (see series 3 in Table 3). The results of these experiments (Table 5) show an increase of $-\ln(\eta_{H_2,G}(30\ \text{min})/\eta_{H_2,G}(0))$ with catalyst concentration.

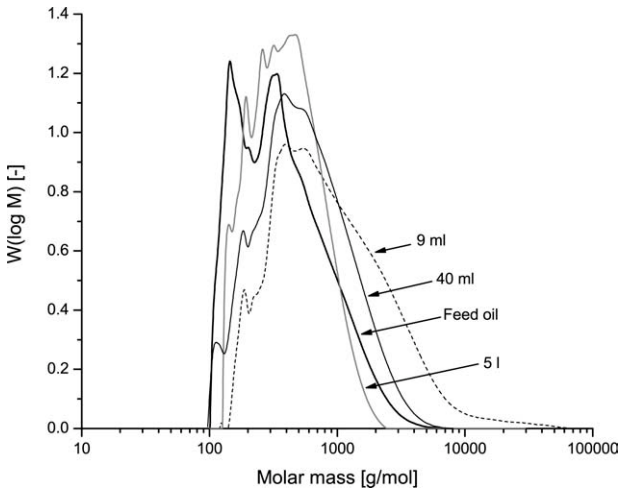

Figure 6. Molecular weight distribution curves of oil products obtained in experiments carried out using the shaken setups with different reactor volumes (9 and 40 ml).

Reaction temperature: 300°C. Reaction time: 30 min. The data for the 5-l experiment (from Ref. 1) correspond to 4-h reaction time (plus ~90-min heating time) at 300°C end temperature.

Table 5. Correlation Between the Catalyst Amount, the Hydrogen Consumption, the Logarithm of the Final/Initial Hydrogen Molar Ratio in the Gas Phase, and the Coking Tendency

Catalyst Amount (wt %)	$-\ln(n_{H_2,G}(30\text{ min})/n_{H_2,G}(0))$	Hydrogen Consumption (mol kg^{-1}_{feed})	Coking Tendency (dry MCRT, wt %)
2.5	1.17	4.53	21.4
5	1.82	5.15	18.1
7.5	1.94	5.64	17.2

Experiments were carried out in the 45-ml stirred autoclave at 300°C and 30-min reaction time and 48 Hz stirring speed.

This dependence is more important at lower catalyst concentrations (from 2.5 to 5 wt %) than at higher (from 5 to 7.5 wt %). Nevertheless, the proportional dependence between $-\ln(\eta_{H_2,G}(30\text{ min})/\eta_{H_2,G}(0))$ and ε_s as expected in a regime governed by mass transfer to the catalyst or apparent kinetics (also for the case that the effectiveness factor $\eta < 1$) did not occur. This indicates that, in these HDO experiments, the results must have been affected by the gas–liquid mass-transfer resistance (Eq. 4). Table 5 additionally shows that the coking tendency of the oil products increased when a lower catalyst holdup was used. This indicates that by reducing the overall rate of the hydrotreating reactions, the overall occurrence of polymerization is favored.

$$N_{H_2} = m.k_s.a_s.C_{H_2,G} = m.k_s.(6.\varepsilon_s/d_p).C_{H_2,G} \quad (2)$$

$$N_{H_2} = m.\eta.k_1.\varepsilon_s.C_{H_2,G} \quad (3)$$

$$N_{H_2} = m.k_L.a_{GL}.C_{H_2,G} \quad (4)$$

Mass-transfer limitations during HDO

$k_L.a_{GL}$ Estimation. To be able to explain the results obtained at various stirring speed, an estimation of the dependence of $k_L.a_{GL}$ on stirring speed in the reactor is needed. Data on $k_L.a_{GL}$ were obtained using absorption of CO_2 in water as nonreactive model system (series 4 in Table 3). The choice of CO_2/water as model system was preferred over H_2/water or H_2/pyrolysis oil because of the low solubility of H_2 in water and the lack of accurate physical solubility data of H_2 in pyrolysis oil, respectively. Moreover, a low temperature was used to obtain a low water vapor pressure, making an accurate monitoring of the relatively small pressure decrease because of physical absorption possible. It should be noted that temperature typically increases $k_L.a_{GL}$ because it reduces the viscosity and surface tension of the liquid (see, for example, Ref. 16).

The gas–liquid mass-transfer experiments were interpreted using well-known theories for gas absorption.[17] The experimentally derived $k_L.a_{GL}$ values are given in Figure 7. Although these $k_L.a_{GL}$ data are only indicative for actual experimental HDO conditions (pyrolysis oil, high temperature and pressure), they strongly indicate that, in this setup, variation of the stirring rate from 7 to 48 Hz causes a substantial (order of magnitude) change in $k_L.a_{GL}$.

Influence of Stirring Speed on the Competing Reactions. Experiments were carried out in the 45-ml stirred autoclave using various stirring rates at 300°C, a reaction time of 30 min, a catalyst concentration of 5 wt %, and an initial hydrogen pressure of 12 MPa (series 5, Table 3). Figure 8a gives the MWD of the oil products, showing that heavier products were obtained when decreasing the stirring intensity. At the same time, H_2 consumption increased with stirring speed (Figure 8b). This shows that with decreasing stirring speed and, thus, $k_L.a_{GL}$, polymerization reactions were increasingly favored over hydrotreating reactions. Thus, the gas–liquid mass-transfer resistance (Eq. 4) appears to be important in the competition between polymerization and hydrotreating reactions in the early stage of the HDO process. The maximum hydrogen consumption observed (at 48 Hz) in 30 min at 300°C was 5.2 mol kg^{-1}_{feed}. This hydrogen consumption in only 30 min (early stage of HDO) is substantial when compared with the consumption in the 5-l autoclave and 5.5 h of reaction time (11.7 mol kg^{-1}_{feed}). This also indicates that in the early stage of the HDO process, hydrogen-consuming reactions can be (very) fast. In the next section, this is also quantitatively verified.

It is also interesting to observe how the CO_2 production (typically observed during HPTT of pyrolysis oil[9]) increased with a decrease in stirring speed (Figure 8b). In a previous study on HDO,[15] CO_2 production also increased upon a shortage of hydrogen. These findings suggest that not only in HPTT but also in HDO, the extent of CO_2 production is related to the extent of polymerization reactions.

When comparing the $k_L.a_{GL}$ and the $-\ln(\eta_{H_2,G}(30\text{ min})/\eta_{H_2,G}(0))$, a proportional dependence should be observed if the gas–liquid mass transfer would control the hydrogen uptake (rate). Table 6 shows that at low stirring speeds (under 15 Hz), this dependence is significant and more than proportional. It should be taken into account that part from the hydrogen consumption might originate from presaturation of the liquid, and, moreover, the $k_L.a_{GL}$ values used are only indicative. However, at the 48 Hz, the linearity is not present anymore, indicating that other mass-transfer or kinetic resistances are also taking place. These results are consistent with those obtained using different catalyst holdups, in which the change of catalyst holdup

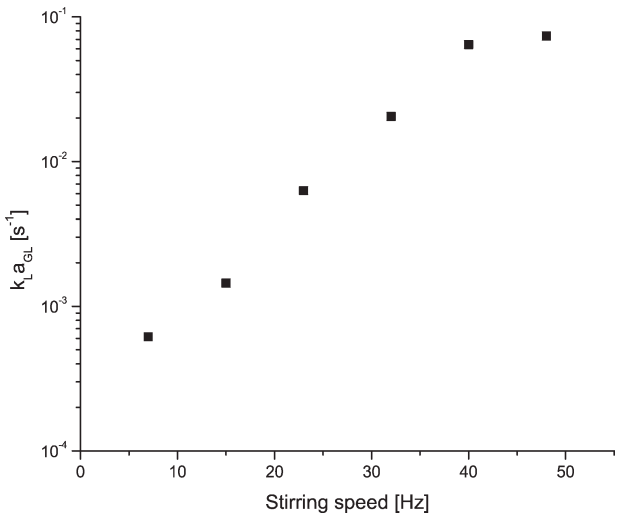

Figure 7. $k_L.a_{GL}$ values for stirring speeds from 7 to 48 Hz at 20°C in the stirred 45-ml autoclave, determined by CO_2 physical absorption in water.

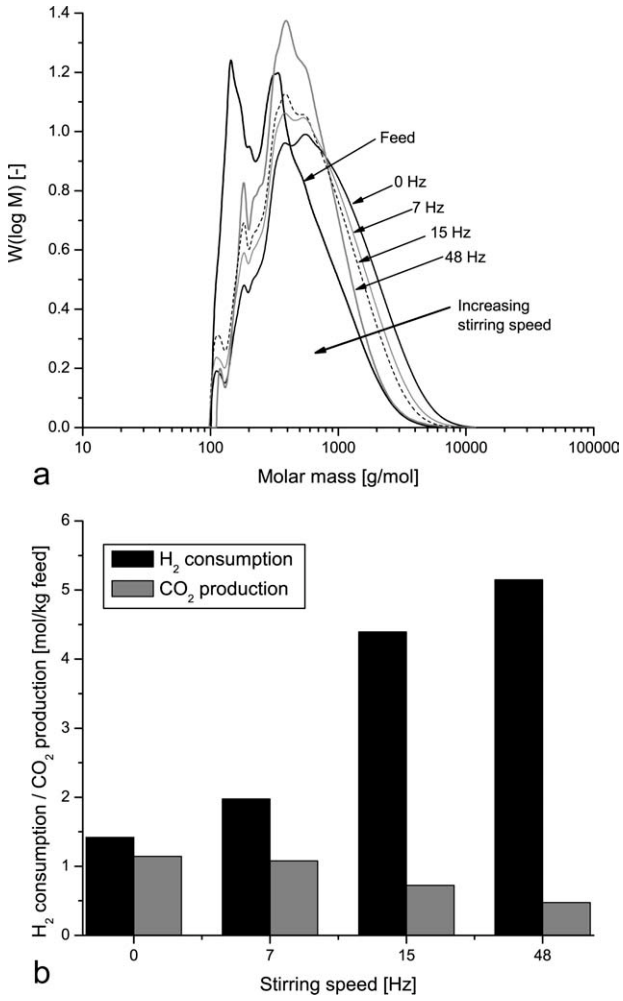

Figure 8. (a) Molecular weight distribution of the oil products obtained at different stirring speeds; experiments were carried out in the 45-ml stirred autoclave at 300°C for 30 min using 5 wt % catalyst; (b) H_2 consumption and CO_2 production for the same experiments.

at low values had stronger effect on the hydrogen consumption than when changed within high values.

Rate-Controlling Step. In the previous sections, it has been shown that neither the mass transfer (Eqs. 2 and 4) nor the apparent kinetics (Eq. 3) is the only controlling step in the hydrotreating reactions, at least for the whole reaction time of 30 min. In this section, the hydrogen consumption rate in subsequent time intervals is analyzed to evaluate the importance of each resistance in these time intervals. First, the two mass-transfer terms in Eq. 1 are compared, assuming that the apparent kinetics is very fast and not limiting. This would reduce Eq. 1 to

$$N_{H_2} = \frac{C_{H_2,G}}{\frac{1}{m.k_L.a_{GL}} + \frac{1}{m.k_S.a_S}} \ (\text{mol m}^{-3}_{\text{liquid}}\ \text{s}^{-1}) \qquad (5)$$

As the distribution coefficient m is present in both resistances, it is only necessary to compare $k_L.a_{GL}$ to $k_S.a_S$ to indicate which of these mass-transfer resistances is more important. Based on the conservative assumption of a Sherwood number of 2 and a diffusivity of H_2 in water at room temperature of $4.6\cdot\times\ 10^{-9}$ m^2 s^{-1} (Ref. 18) (which would be higher at higher temperature), k_S is estimated to be at least $6.5\cdot\times\ 10^{-4}$ m s^{-1}. To calculate a_S, the catalyst holdup (ε_s) is needed, which is $\sim$0.046 $m^3_{catalyst}$ $m^{-3}_{liquid.}$* This gives an a_S of $1.98\cdot\times\ 10^4$ $m^2_{catalyst}$ m^{-3}_{liquid}, resulting in a $k_S.a_S$ of 12.95 s^{-1}. This value is more than two orders of magnitude higher than the $k_L.a_{GL}$ values as reported in this study (Figure 7). Therefore, in this study, Eq. 5 can be further simplified to

$$N_{H_2} = m.k_L.a_{GL}.C_{H_2,G} \qquad (6)$$

It should be noted that, in the derivation of Eq. 6, it has been assumed that apparent kinetics was not limiting, whereas for the actual experiments shown in the previous section some influence of the catalyst holdup was observed for 30-min reaction time. Because $k_S.a_S$ has proven not to be limiting, it can be concluded that the influence of catalyst holdup in the previous section was due to the apparent kinetic term (Eq. 3). This also means that actual $k_L.a_{GL}$ values will be at least equal to or higher than the ones derived using experimental fluxes and Eq. 6. In Table 7, the experimental hydrogen consumption rate for two time intervals is shown. These intervals are from 3 to 5 min (excluding, in this way, large part of the heating time) and from 5 to 30 min (the rest of the experiment). The rate was determined from the change in reactor pressure in time (subtracting the water vapor pressure at the corresponding temperature). The H_2 consumption rate decreased strongly with the reaction time. The last column in Table 7 shows the calculated H_2 consumption rate as if the liquid-side mass transfer was the rate-controlling step using Eq. 6. Considering the uncertainty in the estimates used in the calculations (among others $k_L.a_{GL}$, m, pyrolysis oil density), the theoretically predicted gas–liquid mass-transfer rate agrees well with the experimentally observed hydrogen consumption rate for the period of 3–5 min. However, the measured average hydrogen consumption rate for the period of 5–30 min is much lower than the maximum mass-transfer flux predicted using Eq. 6. These findings indicate that in the first period of reaction process (3–5 min), gas–liquid mass transfer is to a large extent limiting the overall hydrogen consumption rate, but its importance decreases with time/conversion. The hydrogen consumption rate at/inside the catalyst (governed by apparent kinetics, see Eq. 3) is expected to become more important in this second period (5–30 min). A reason for this behavior might be that because of the fast heating to high temperatures many pyrolysis oil components become reactive toward

Table 6. Correlation Between the $k_L.a_{GL}$ and the Final/ Initial Hydrogen Molar Ratio in the Gas Phase

Stirring Speed (Hz)	$k_L.a_{GL}$	$-\ln(n_{H_2,G}(30\ \text{min})/n_{H_2,G}(0))$
0	0	0.24
7	6.17×10^{-4}	0.36
15	1.44×10^{-3}	1.09
48	7.35×10^{-2}	1.82

Experiments were conducted in the 45-ml autoclave at 300°C, 30 min, and 5 wt % catalyst.

*In the experiment, 20 g of liquid (16.7 cm^3) and 1 g of catalyst ($\sim$0.77 cm^3, by using a skeletal density of 2 g cm^{-3} (Refs. [19] and [20]) and porosity of 0.27 cm^3 g^{-1}) were used.

Table 7. Estimated Average H_2 Consumption Rates and Temperatures at Different Time Intervals for the Experiment in the Stirred 45-ml Autoclave

Time Interval (min)	Measured Average H_2 Consumption Rate (mol min^{-1} kg_{feed})	Measured Average H_2 Consumption Rate (mol $s^{-1}m^3_{feed}$)*	Average Temperature in Time Interval (Range) (°C)	Distribution Coefficient† (m)	Average H_2 Concentration in the Gas in the Time Interval,‡ $C_{H_2,G}$ (mol m^{-3})	Predicted H_2 Consumption Rate Assuming Overall G-L Limitation§ (mol s^{-1} m^3_{feed})
3–5	0.61	12.1	265 (248–276)	0.087	2058	13.2
5–30	0.06	1.2	289 (277–290)	0.122	908	8.2

5 wt % catalyst, 300°C end temperature, 30 min total, and H_2 initial pressure of 12 MPa.
*Because the changes in density of pyrolysis oil are not known, the density at room temperature (1200 kg m^{-3}) was used.
†Estimated by interpolation data from distribution coefficients for H_2 in water at different temperatures.[21]
‡From estimated H_2 partial pressure in reactor.
§Using Eq. 6; $m_{H_2,G\text{-water}}$ from Ref. 21, $C_{H_2,G}$ from the average H_2 partial pressure (in the interval) and Soave-Redlich-Kwong equation of state, and the $k_L.a_{GL}$ (measured in the CO_2/water model system) at 48 Hz from Figure 8.

hydrotreating at the same time.[6] This requires a large flux of hydrogen, resulting in depletion of hydrogen in the liquid and, thus, gas–liquid mass-transfer limitations in the early stage of HDO. Slower and gradual heating, like used in the 5-l autoclave experiments,[1] would probably avoid this.

Estimations for industrial reactors

Previous sections showed that gas–liquid mass-transfer resistances are likely to be important during the initial period of the HDO process (3–5 min), especially for experiments carried out above 200°C. The model reactors as used in this study typically have high specific energy input and, thus, good mass-transfer characteristics when compared with industrial reactors. It is, therefore, likely that gas–liquid mass-transfer resistances also play an important role in industrial application, especially during the early stage of the HDO process. Other resistances can become of much more importance in industrial reactors because of the use of larger particles: these include not only extraparticle but also intraparticle mass-transfer resistances (in this study, the catalyst particle size was very small). It should be kept in mind that even when mass-transfer characteristics are (very) good, the intrinsic kinetics, the catalyst holdup, and degree of utilization (or effectiveness factor) of the catalyst should also be such that overall the hydrotreating reactions are favored over the polymerization reactions. An estimate on the degree of utilization for larger particle sizes than used in this study will be given based on current experimental data.

The previous section has shown that in an initial period (<5 min) at a temperature of 300°C liquid-side mass transfer is likely to be controlling the overall hydrogen consumption rate. The following equation can thus be postulated

$$N_{H_2,3-5\ min,experimental} < m.\eta.k_{1,3-5\ min}.\varepsilon_s.C_{H_2,G} \qquad (7)$$

Using Eq. 7 will thus yield a lower boundary for $k_{1,3-5\ min}$. Because only one particle size was used in this study (14 μm), the actual degree of utilization, η, could not be determined. To estimate η for larger particle sizes than the one used in this study, it was additionally assumed that η (14 μm) = 1. This enables the calculation of a "lower–lower" boundary for k_1 (using Eq. 7) and, thus, estimation of η_{max} for larger particles. Using the measured H_2 consumption rate in the period of 3–5 min, the estimated H_2 distribution coefficient, and average H_2 concentration in the same interval (see Table 7), the kinetic rate constant in this period is estimated to be $k_{1,3-5\ min} \geq 1.46$ s^{-1}. Again, this only gives a lower boundary for the kinetic constant in this time period as it has been shown that gas–liquid mass-transfer limitations were present, and η (14 μm) was assumed to be unity.

With $k_{1,3-5\ min}$ known and using the Thiele modulus ($\phi = (d_p/6).\sqrt{k_I/D_{eff}}$), the degree of utilization ($\eta = \tanh\ \phi/\phi$) can be calculated for different particle sizes. D_{eff} was estimated by using the diffusivity of H_2 in water corrected by the porosity of the catalyst particle (ε) and a tortuosity factor (τ) ($D_{eff} = \varepsilon.D_{H_2}/\tau$). For the catalyst used, the porosity was 0.27 cm^3 g^{-1}, but the tortuosity was not known. Typically, τ has a value between 2 and 5.[22] Therefore, an intermediate value of 0.1 for the ε/τ was taken. Figure 9 shows the influence of the particle size (industrial hydrogenation reactors use catalyst particles with a size up to

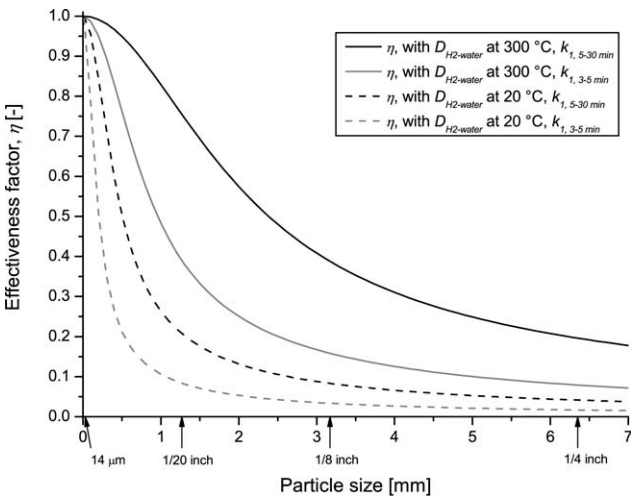

Figure 9. Estimate of (maximum) effectiveness factor (or degree of utilization) of a Ru/C catalyst particle of HDO process (300°C) as a function of catalyst particle size.

The dotted lines correspond to values calculated using the diffusivity of H_2 in water at 20°C. The solid lines use an approximation of the diffusivity by correcting the diffusivity at 20°C by temperature and viscosity (using the Einstein–Stokes correlation, $D_{H_2,20°C} = 5.11\cdot\times\ 10^{-9}$ m^2 s^{-1}, $D_{H_2,300°C} = 1.02\cdot\times\ 10^{-7}$ m^2 $s^{-1} = (\mu/T)_{20°C}/(\mu/T)_{300°C}$ $D_{H_2,20°C}$). The gray lines correspond to the effectiveness factor at the initial period of reaction (3–5 min) and the black lines to the later period (5–30 min).

1/4 inch[23]) on the degree of utilization. Because the degree of utilization is affected by diffusivity, and the diffusivity of H_2 in water at high temperature is not known, it was estimated using the Einstein–Stokes correlation. The figure shows that even with the estimated higher diffusivity, increasing the particle size would reduce the (maximum) degree of utilization significantly below 1. When the same calculation procedure is repeated for the interval of 5–30 min, $k_{1,\ 5\text{–}30\ \mathrm{min}}$ is calculated to be 0.24 s^{-1}. In Figure 9, the estimated degree of utilization for this reaction rate constant is also shown. Although higher than for the initial period of the experiment, also in this case it is significantly below 1. This can again affect the ratio of the hydrogenation to the polymerization reactions in the early stage of the HDO process and therewith influence product quality if not properly accounted for. It should be noted that these findings not only apply to the design of industrial reactors but also to the screening of HDO catalyst using pyrolysis oils. In these studies, care should be taken that polymerization is not governing as this would result in similar apparent (low) catalyst activity. Even if this condition is fulfilled, polymerization cannot be ruled out, and a meaningful comparison of apparent catalyst activity is, thus, only possible if similar process conditions are applied (like catalyst size and holdup, mass-transfer characteristics, and heating rate).

Conclusions

The competition between polymerization and hydrotreating reactions occurring during the early stage of pyrolysis oil HDO has been studied using near isothermal, intensively mixed reactors. The aim was to identify process conditions that are of influence on this competition in order to be able to minimize polymerization reactions that typically lead to undesirable product properties.

Low temperatures favored hydrotreating reactions. However, if the heating rate to temperatures above 200–250°C was fast, not giving enough time to the hydrotreating reactions below these temperatures to occur, polymerization quickly took place creating a product refractive toward hydrotreating.

Experiments carried out at 300°C using different stirring speeds showed that total hydrogen consumption increased with stirring speed, whereas the extent of polymerization decreased (measured by the MWD of the oil product and CO_2 production). This indicates that gas–liquid mass-transfer limitations were occurring. Increasing the catalyst holdup reduced the extent of polymerization and increased the hydrogen uptake (although less than proportional), indicating that intraparticle/kinetic resistances also played a role in the experiments.

Calculations on the hydrogen consumption rates for various time intervals in a 30-min experiment at 300°C (high intensity stirring) showed high consumption rates in the initial period (under 5 min) and lower rates afterward. Using estimations on the mass-transfer coefficients, the gas–liquid mass transfer appeared to be the controlling step during the initial period. Afterward, the intraparticle/kinetic resistances gained importance.

Indicative calculations on the effect of catalyst size showed that, in the early stage of HDO process, the expected degree of utilization for particle sizes typically used in industrial fixed bed reactors is below unity.

This work has shown that hydrotreating reactions can be favored over polymerization reactions by selecting adequate reactor (good mixing), catalyst (small particles), and process conditions (enough time at low temperature). Insights obtained in this study can help in the design of industrial HDO reactors.

Acknowledgments

The authors acknowledge the EU for partial funding of the work through the BIOCOUP project within the 6th Framework Program (contract number: 518312) and the CORAF project of Senter Novem (project number EOSLT04018).

Notation

a_{GL} = gas–liquid interface area ($m^2_{interface}\ m^{-3}_{liquid}$)
C_1 = $(1/((d_p/(6.m.k_s)) + (1/m.\eta.k_1))).(1/V_G)$
a_S = catalyst area per unit of liquid volume: $6.\varepsilon_s/d_p$ ($m^2_{catalyst}\ m^{-3}_{liquid}$)
$C_{H_2,G}$ = concentration of hydrogen in the gas phase (mol m^{-3}_{gas})
$C_{H_2,L}$ = concentration of hydrogen in the liquid phase (mol m^{-3}_{liquid})
D_{eff} = effective diffusivity ($m^2\ s^{-1}$)
$C_{H_2,L}$ = diffusivity of hydrogen in a liquid ($m^2\ s^{-1}$)
d_p = particle size/diameter (m)
E_a = activation energy (kJ mol^{-1})
GPC = gel permeation chromatography
HDO = hydrodeoxygenation
HPTT = high-pressure thermal treatment
k_0 = Arrhenius constant (s^{-1})
k_1 = reaction rate constant for hydrogen-consuming reactions (s^{-1})
k_{HPTT} = reaction rate constant for HPTT gas formation (s^{-2})
k_L = gas–liquid mass-transfer coefficient ($m^3_{liquid}\ m^{-2}_{interface}\ s^{-1}$)
k_S = liquid–solid mass-transfer coefficient ($m^3_{liquid}\ m^2_{catalyst}\ s^{-1}$)
m = distribution coefficient (from Henry's law): $(C_{H_2,L}/C_{H_2,G})_{at\ equilibrium}$
MCRT = microcarbon residue test
MW = molecular weight
MWD = molecular weight distribution
n_{H_2} = hydrogen moles
N_{H_2} = hydrogen molar flux (mol $m^{-3}_{liquid}\ s^{-1}$)
R = gas constant: 8.314 (J $mol^{-1}\ K^{-1}$)
Re = Reynolds number: $d_p.v.\rho.\mu^{-1}$, from Ref. 24
Sc = Schmidt number: $\mu.\rho.D^{-1}$, from Ref. 24
Sh = Sherwood number: $2 + Re^n + Sc^m = k_S.d_p.D^{-1}$, from Ref. 24
T = time (s)
T = temperature (K)
V = velocity (m s^{-1})
V_G = gas volume (m^3_{gas})

Greek letters

ε = porosity ($m^3_{pore}\ g^{-1}_{catalyst}$)
ε_s = catalyst holdup ($m^3_{catalyst}\ m^{-3}_{liquid}$)
ϕ = Thiele modulus: $(d_p/6).k_1^{1/2}.D_{eff}^{-1/2}$
η = effectiveness factor or degree of utilization of a porous catalyst: $(\tanh\ \phi)\phi^{-1}$.
μ = viscosity (Pa s)
ρ = density (kg m^{-3})
τ = tortuosity factor

Literature Cited

1. De Miguel Mercader F, Groeneveld MJ, Kersten SRA, Way NWJ, Schaverien CJ, Hogendoorn JA. Production of advanced biofuels: co-processing of upgraded pyrolysis oil in standard refinery units. *Appl Catal B Environ*. 2010;96:57–66.
2. French RJ, Hrdlicka J, Baldwin R. Mild hydrotreating of biomass pyrolysis oils to produce a suitable refinery feedstock. *Environ Prog Sustain Energy*. 2010;29:142–150.

3. Fogassy G, Thegarid N, Toussaint G, van Veen AC, Schuurman Y, Mirodatos C. Biomass derived feedstock co-processing with vacuum gas oil for second-generation fuel production in FCC units. *Appl Catal B Environ*. 2010;96:476–485.
4. Elliott DC. Historical developments in hydroprocessing bio-oils. *Energy Fuels*. 2007;21:1792–1815.
5. Elliott DC, Baker EG. Process for upgrading biomass pyrolyzates. US Patent 4,795,841, 1989.
6. Laurent E, Pierret C, Grange P, Delmon B. Control of the deoxygenation of pyrolytic oils by hydrotreatment. In: *Proceedings of the 6th Conference on Biomass for Energy, Industry and Environment*, Athens, Greece,1991:665–671.
7. Elliott DC, Neuenschwander GG. *Liquid fuels by low-severity hydrotreating of biocrude*. In: Bridgwater AV, Boocock DGB, editors. *Developments in Thermochemical Biomass Conversion*. London: Blackie Academic & Professional,1996:611–621.
8. Venderbosch RH, Ardiyanti AR, Wildschut J, Oasmaa A, Heeres HJ. Stabilization of biomass-derived pyrolysis oils. *J Chem Technol Biotechnol*. 2010;85:674–686.
9. De Miguel Mercader F, Groeneveld MJ, Kersten SRA, Venderbosch RH, Hogendoorn JA. Pyrolysis oil upgrading by high pressure thermal treatment. *Fuel*. 2010;89:2829–2837.
10. Zhang S, Yong-Jie Y, Li T, Ren Z. Study of hydrodeoxygenation of bio-oil from the fast pyrolysis of biomass. *Energy Source*. 2003;25: 57–65.
11. Sheu Y-HE, Anthony RG, Soltes EJ. Kinetic studies of upgrading pine pyrolytic oil by hydrotreatment. *Fuel Process Technol*. 1988; 19:31–50.
12. Zhang S, Yan Y, Li T, Ren Z. Lumping kinetic model for hydrotreating of bio-oil from the fast pyrolysis of biomass. *Energy Source A*. 2009;31:639–645.
13. Voorhoeve RJH, Stuiver JCM. Kinetics of hydrogenation on supported and bulk nickel-tungsten sulfide catalysts. *J Catal*. 1971;23: 228–235.
14. Guo H, Li H, Xu Y, Wang M. Liquid phase glucose hydrogenation over Cr-promoted Ru-B amorphous alloy catalysts. *Mater Lett*. 2002;57:392–398.
15. De Miguel Mercader F, Groeneveld MJ, Kersten SRA, Geantet C, Toussaint G, Way NWJ, Schaverien CJ, Hogendoorn JA. Hydrodeoxygenation of pyrolysis oil fractions. Process understanding and quality assessment through co-processing in refinery units. *Energy Environ Sci*. DOI: 10.1039/c0ee00523a. In press.
16. Zieverink MMP, Kreutzer MT, Kapteijn F, Moulijn JA. Gas-liquid mass transfer in benchscale stirred tanks fluid properties and critical impeller speed for gas induction. *Ind Eng Chem Res*. 2006;45: 4574–4581.
17. Cents AHG, Brilman DWF, Versteeg GF. Mass-transfer effects in the biphasic hydroformylation of propylene. *Ind Eng Chem Res*. 2004;43:7465–7475.
18. *Handbook of Chemistry and Physics*, 84th ed. David R. Lide, author/ed., Boca Raton: CRC Press, 2003.
19. Agarwal RK, Noh JS, Schwarz JA, Davini P. Effect of surface acidity of activated carbon on hydrogen storage. *Carbon*. 1987;25: 219–226.
20. Agarwal RK, Schwarz JA. Analysis of high pressure adsorption of gases on activated carbon by potential theory. *Carbon*. 1988;26: 873–887.
21. Baranenko VI, Kirov VS. Solubility of hydrogen in water in a broad temperature and pressure range. *Atom Energy*. 1989;66:30–34.
22. Van Santen RA, van Leeuwen PWNM, Moulijn JA, Averill BA. *Catalysis: An Integrated Approach*, 2nd ed. Amsterdam: Elsevier Science BV, 2000.
23. Sanfilippo D, Rylander PN, editors. In: *Ullmann's Encyclopedia of Industrial Chemistry*. 6th ed., Vol. 17. Wiley-VCH 2002:241–252.
24. Harriott P. *Chemical Reactor Design*. New York: Marcel Dekker, 2003.

Manuscript received Oct. 4, 2010, and revision received Nov. 19, 2010.